



## RESEARCH ARTICLE

# The effect of acupuncture on hippocampal synaptic plasticity in Alzheimer Disease Mouse Model: Possible mechanisms of energy transportation in neurons

Chang-le Wu<sup>1,†</sup>, Meng-jing Wang<sup>1,†</sup>, Xiao-shu Zhang<sup>2</sup>, Li Zhang<sup>1</sup>, Yi-yun Yuan<sup>1</sup>, Ping Du<sup>3</sup>, Min Feng<sup>4\*</sup>, Shu-guang Yu<sup>3\*</sup>, Qi Liu<sup>1\*</sup>

<sup>1</sup>College of Acupuncture-Moxibustion and Tuina, Shaanxi University of Chinese Medicine, Xi'an 712046, China

<sup>2</sup>Huaqiao University Hospital, Quanzhou 362021, China

<sup>3</sup>College of Acupuncture-Moxibustion and Tuina, Chengdu University of Traditional Chinese Medicine, Chengdu 610075, China

<sup>4</sup>Department of Rehabilitation and Healthcare, Hunan University of Medicine, Huaihua 418000, China

<sup>†</sup>These authors contributed equally to this manuscript.

\*[fengminfengmin@sina.com](mailto:fengminfengmin@sina.com)

\*[ysg@cdutcm.edu.cn](mailto:ysg@cdutcm.edu.cn)

\*[lq6677@sntcm.edu.cn](mailto:lq6677@sntcm.edu.cn)



## PUBLISHED

30 August 2024

## CITATION

Wu, Cl., et al., 2024. The effect of acupuncture on hippocampal synaptic plasticity in Alzheimer Disease Mouse Model: Possible mechanisms of energy transportation in neurons. *Medical Research Archives*, [online] 12(8).

<https://doi.org/10.18103/mra.v12i8.5739>

## COPYRIGHT

© 2024 European Society of Medicine. This is an open-access article distributed under the terms of the Creative Commons Attribution License, which permits unrestricted use, distribution, and reproduction in any medium, provided the original author and source are credited.

## DOI

<https://doi.org/10.18103/mra.v12i8.5739>

## ISSN

2375-1924

## ABSTRACT

**Objective:** To study the mechanism of acupuncture-promoted synaptic plasticity in hippocampal neurons of senescence-accelerated mouse-prone 8 mice with respect to neuronal energy substrate transport.

**Methods:** Forty-three senescence-accelerated mouse-prone 8 mice were randomly divided into Alzheimer's disease model and acupuncture groups, and twenty senescence-accelerated mouse resistant 1 mice were used as the normal group. Acupuncture group received acupuncture at the "Baihui" and "Yongquan" acupoints for 40 days. The Morris water maze was used to detect the learning and memory capabilities of the mice, and in vivo electrophysiology and transmission electron microscopy were used to evaluate the synaptic functional and structural plasticity of hippocampal neurons. Glucose, lactate, and pyruvate in the hippocampal intercellular fluid, as well as the expression of glucose transporter 3 and monocarboxylate transporters 2 and 4, were analyzed using microdialysis, immunohistochemistry, and western blotting.

**Results:** The Morris water maze data showed that compared with Alzheimer's disease model mice, mice of acupuncture group exhibited a shorter escape latency, increased number of effective zone crossings, and increased percentage of swimming distance in the target quadrant. Acupuncture increased the postsynaptic density thickness of Alzheimer's disease model mice and decreased the latency amplitude after tetanic stimulation and width of the synaptic cleft. Glucose, lactate, and pyruvate contents in the hippocampal intercellular fluid were significantly reduced in Alzheimer's disease model mice, but the reductions were more pronounced after acupuncture treatment. Furthermore, acupuncture prominently elevated glucose transporter 3 and monocarboxylate transporters 2 expression in the CA1 and dentate gyrus regions of the hippocampus of Alzheimer's disease model mice. The elevation of monocarboxylate transporters 4 expression mostly appeared in the CA1 region.

**Conclusion:** Acupuncture improved the learning and memory capabilities as well as the hippocampal synaptic structural plasticity of senescence-accelerated mouse-prone 8 mice. Its effects were likely related to the regulation of glucose transporter 3, monocarboxylate transporters 2, and monocarboxylate transporters 4 expression in the hippocampal tissue to increase the energy substrate reserve of neurons and improve the substrate-matching ability of the cellular response.

**Keywords:** acupuncture; Alzheimer's disease; synaptic plasticity; neuronal energy substrate transport

## Introduction

Alzheimer's disease (AD), a degenerative disease of the central nervous system (CNS), is predominant in the older population and is accompanied by progressive memory and cognitive impairments. The main pathological features include amyloid-beta ( $A\beta$ ) plaques and tau protein deposition<sup>1</sup>. The hippocampus is a key area of early damage in AD<sup>2</sup>; specifically, impairment of hippocampal synaptic plasticity is a pathological mechanism of AD<sup>3-4</sup>. Additionally, impaired neuronal energy metabolism related to  $A\beta$  in the brain is an early event in AD and a common pathway leading to neuronal degeneration<sup>5-6</sup>, and the degree of reduced glucose metabolism in the brain is proportional to the level of reduced learning and memory capacity in AD<sup>7</sup>. As is well-known, neuronal energy metabolism substrates are formed not only by glucose, but also by lactate and pyruvate<sup>8</sup>. Lactate transportation among astrocytes–neurons is essential for maintaining long-term potentiation (LTP) and forming long-term memory<sup>9</sup>, and is crucial for energy metabolism in the pathophysiological states of the nervous system<sup>10</sup>. However, different energy substrates must be transported from the blood to the brain interstitial fluid (BIF) and neurons using glucose transporters (GLUTs) and monocarboxylate transporters (MCTs)<sup>7,11</sup>. GLUT3 is distributed in neurons and is the main glucose transporter from the extracellular matrix into the neurons<sup>12</sup>. MCTs are responsible for transporting monocarboxylic acids such as lactate and pyruvate, of which MCT4 is mainly expressed in astrocytes, whereas MCT2 is primarily expressed in neurons<sup>11,13</sup>. Therefore, the level of transporter protein expression directly determines the efficiency of substrate uptake by neurons, and probably affects the functional activity of neurons associated with learning and memory.

Previous clinical and experimental studies have proven the therapeutic effects of acupuncture treatment in AD<sup>14-18</sup>. Acupuncture can improve the learning and memory capabilities in animal models of AD, and has benign regulatory effects on mitochondrial ultrastructure, mitochondrial respiratory

chain enzyme activity, and lactate in hippocampal neurons of senescence-accelerated mouse-prone 8 (SAMP8) mice, while promoting synaptic structural plasticity. These results confirm that acupuncture effectively improves energy metabolism in the brains of SAMP8 mice and promotes synaptic plasticity of hippocampal neurons. However, it is still unclear whether the promotion of hippocampal neuronal synaptic plasticity by acupuncture treatment is related to the substrate transportation of energy metabolism. Thus, in this study, we explored the possible mechanisms of acupuncture-promoted synaptic plasticity from the roles of neurons and astrocytes in energy substrate transportation in the AD brain using neuron-specific GLUT3 and MCT2 and astrocyte-specific MCT4 transporters as the entry points.

## Materials and methods

### ANIMAL GROUPS

This study was conducted in compliance with the Regulations on the Administration of Animal Experiments, issued by the Ministry of Science and Technology of the People's Republic of China, and ethical approval was obtained from the Ethics Committee of Shaanxi University of Chinese Medicine. Sixty male SAMP8 mice and twenty 8-month-old male SAMR1 mice (20±2 g) were purchased from the Animal Center, Laboratory of Senile Encephalopathy, First Affiliated Hospital of Tianjin University of Traditional Chinese Medicine (animal lot: SCXK [Jin] 2008-0001). The mice were individually housed in an environmentally controlled vivarium under a 12 h light-dark cycle (temperature 25±3°C, humidity 40–60%). Food and water were provided *ad libitum*. After a week of adaptive domestication, SAMP8 mice were screened using the Morris water maze (MWM) method, as previously reported<sup>19</sup>. After completing the test, animals with visual, motor, and sensory impairments were excluded. The remaining 53 SAMP8 mice were randomly divided into two groups: AD (n=27) and acupuncture (A) (n=26) groups. All 20 SAMR1 mice were included in normal (N) group.

## ACUPUNCTURE TREATMENT

In Group A, the “Baihui” (GV20) and “Yongquan” (K11) acupoints, which showed some improvement in learning and memory ability<sup>14,15,20</sup>, were selected for treatment. The locations of these acupoints were based on the “Atlas of Animal Acupuncture Points” developed by the Experimental Acupuncture Branch of the Chinese Acupuncture and Moxibustion Society. After local skin disinfection on the acupoints, disposable sterile acupuncture needles (0.19 mm × 10 mm) (Suzhou Medical Supplies Factory, Jiangsu, China) were inserted 2–3 mm into the “Baihui” and “Yongquan” points forward and backward, respectively, and the needles were retained for 20 minutes. During this period, the twisting method was used to perform mild reinforcing-attenuating acupuncture once every 5 minutes, with a frequency of 150 times/min and a duration of 10 seconds/time. The bilateral “Yongquan” points were alternately needled daily. Mice in the N and AD groups received only grasping and fixation without acupuncture. Grasping, fixation, and acupuncture treatments were performed by the same operator. Acupuncture treatment (20 min/ session, 1 time/day) lasting for 5 days was considered as one treatment course, and eight courses were performed with an interval of 2 days between each session.

## MWM TEST

The test was conducted as previously reported<sup>19</sup>. After performing acupuncture, a 5-day place navigation test (PNT) and the 1-day spatial probe test (SPT) were performed in each mice group to evaluate their learning and memory capabilities. The criteria for evaluation included the time from placement in the water to finding the platform (escape latency), number of effective zone crossings, and percentage of swimming distance in the target quadrant. Swimming distance was automatically monitored by a video camera mounted on the ceiling of the room. All data were analyzed using Watermaze software (Taimeng Ltd, Chengdu, China).

## IN VIVO ELECTROPHYSIOLOGY MEASUREMENT OF HIPPOCAMPAL LTP

Electrophysiological tests have been used to evaluate changes in synaptic functional plasticity<sup>20</sup>. Randomly

chosen mice from each group (n=5 in group N, n=6 in groups AD and A) were anesthetized with urethane (1.5 g/kg) and fixed in a stereotaxic apparatus (Stoelting, USA). By referring to the stereotaxic atlas<sup>21</sup>, the corresponding area of the skull was drilled. The signal recording electrode was slowly inserted into the dentate gyrus (DG) granule cell layer of the hippocampus, the stimulating electrode was inserted into the front perforant path (PP), and the reference electrode was clamped to the scalp. The stimulator parameters were adjusted to a wave width of 100 μs and current of 0.3 mA to induce a population spike (PS). Then, the stimulation and recording electrodes were adjusted to obtain an optimal PS, and the stimulation intensity was adjusted to 1/3–1/2 of the maximum PS value after 60 min. After PS was recorded for 30 min as the baseline, tetanic stimulation (TS) was administered to induce LTP. Each string of TS consisted of five pulse waves with a frequency of 150 Hz and width of 150 μs. Eight strings were administered at an interval of 10 s. Next, PS was recorded for 60 min after three TS cycles. The recorded signals were amplified and converted using a microelectrode amplifier (Axoclamp 2B; Axon Instruments, USA) and digital-to-analog converter (Digidata 1322A; Axon Instruments), respectively. Finally, the amplitude changes in PS and latency after TS (%) were analyzed using the WinLTP Software (University of Bristol, England, UK). The ratio of the PS and latency evoked by each single-pulse test stimulus (with the same parameters as the baseline period) after TS to the baseline value was the amplitude change. LTP was defined as at least a 120% increase in the average PS amplitude and was maintained for a minimum of 30 min compared to the baseline value.

## TRANSMISSION ELECTRON MICROSCOPY OBSERVATION AND MEASUREMENT OF HIPPOCAMPAL SYNAPSE

Transmission electron microscopy (TEM) was conducted to observe the ultrastructure of hippocampal synapses in each group<sup>14</sup>. After the MWM test, all mice groups (n=4 per group) were anesthetized with 1% pentobarbital sodium at a concentration of 3 mL/kg. The CA1 region of the left hippocampus was dissected

and trimmed to approximately 1 mm<sup>3</sup> after fixing the perfused brain tissue with 4% paraformaldehyde. Next, the sections were fixed, dehydrated, embedded in Epon812 (Beijing Modern Oriental Fine Chemicals Co. Ltd., Beijing, China), and sectioned (thickness: 100 µm). Finally, the sections were double-stained and observed using TEM (Hitachi H-600IV, Japan). The thickness (nm) of postsynaptic density (PSD), width (nm) of the synaptic cleft, and synaptic curvature were calculated using Image-Pro Plus software (version 6.0; Media Cybernetics, USA) with reference to the synaptic confirmation criteria<sup>22</sup> and stereological formulas<sup>23</sup>.

#### MICRODIALYSIS AND ENERGY SUBSTRATE ASSAY

*Microdialysis* was applied to evaluate changes in lactate, glucose, and pyruvate concentrations in the hippocampal intercellular fluid (HIF) of each mice group. Mice groups (n=6 per group) were anesthetized with 1% sodium pentobarbital (3 mL/kg), and mounted on a stereotaxic instrument (Stoelting) after the MWM test. First, probe catheter embedding was performed in the left hippocampus with reference to the mouse brain stereotaxic atlas (positioning coordinates=anteroposterior: -2.0 mm, mediolateral: 1.5 mm, dorsoventral: 2.0 mm). Three days later, the core of the probe catheter was withdrawn, and the microdialysis probe CMA7 (CMA, Sweden) was inserted into the guide cannula (CMA) to the calibrated depth. Subsequently, using Ringer's solution (Sichuan Kelun Pharmaceutical Co., Ltd., Sichuan, China) as the perfusion fluid, each rat was dialyzed at a constant flow rate of 1 µL/min using a CMA402 Syringe Pump (CMA). The dialysate was collected every 20 min using a MAB 85 Fraction Collector (CMA), and dialysis was continued for 120 min after a 60 min stable phase to obtain six valid samples. Finally, the levels of lactate, glucose, and pyruvate in each dialysate were measured separately using a CMA600 Microdialysis Analyzer (CMA), following the operating instructions of the corresponding kits (Lactate Test Kit, Glucose Test Kit, Pyruvate Test Kit; M Dialysis AB, Sweden).

#### IMMUNOHISTOCHEMISTRY OF ENERGY TRANSPORTERS

In another three randomly selected mice groups (n=7 for groups N and A, n=6 for group AD), the

right hippocampus was isolated and fixed in 4% paraformaldehyde, and dehydration and paraffin embedding were performed after 24 h. The tissues were individually dewaxed, rehydrated, and processed by coronal sectioning (thickness: 10 µm). The sections were incubated with 3% hydrogen peroxide for 10 min at room temperature to deactivate the endogenous enzymes. Then, antigen repair and closure of sections were performed with 0.01 M citrate buffer (pH=6.0) and 5% bovine serum albumin, respectively. Next, the sections were incubated with anti-MCT2 antibody (1:200; AB3542; Millipore, Germany), anti-MCT4 antibody (1:200; AB3314P; Millipore), and anti-GLUT 3 antibody (1:200; AB1344; Millipore), and kept at 4°C overnight. Subsequently, secondary antibody and strept avidin-biotin complex (Beijing Zhongshan Jinqiao Biotechnology Co., Ltd., Beijing, China) were added, and the processed sections were incubated at 37°C for 30 min. Finally, after staining, photographs of the hippocampal CA1, CA3, and DG regions for each section were observed under a microscope with a 400X field of view, and the mean optical density (MOD) values were calculated using Image-Pro Plus software (version 6.0; Media Cybernetics).

#### WESTERN BLOTTING OF ENERGY TRANSPORTERS

The left hippocampus of each mice group (n=7 for groups N and A, n=6 for group AD) was isolated after anesthetization and stored at -80°C. First, the samples were homogenized and centrifuged (4°C, 5 min, 12000 r/min), and the supernatant was collected to evaluate the protein concentration. Equal amounts of protein were separated by electrophoresis and transferred onto polyvinylidene fluoride membranes through electroblotting. The membranes were then blocked with 5% skimmed milk at room temperature for 1 h. Afterward, the membranes of each mice group were incubated overnight at 4°C with the anti-GLUT3 antibody, anti-MCT2 antibody, anti-MCT4 antibody (1:200; Millipore), and beta-actin (EarthOx, USA), respectively. The sections were then washed and incubated with a secondary antibody (Beijing Zhongshan Jinqiao Biotechnology Co., Ltd.) at room temperature for 1 h. Finally, they were exposed and observed, and the target bands were analyzed using

Quantity One software (Bio-Rad, Germany). The ratio of the grayscale of the target protein to that of the internal reference protein was used to determine the relative expression of the target protein.

#### STATISTICAL ANALYSIS

Data are expressed as mean  $\pm$  standard deviation, and all statistical analyses were performed using SPSS software (version 22.0; IBM, Armonk, NY, USA). Escape latency results were analyzed using a repeated-measures analysis of variance (ANOVA), while a one-way ANOVA was conducted on other experimental parameters. Statistical significance was set at  $P < 0.05$ .

## Results

### ACUPUNCTURE IMPROVED LEARNING AND MEMORY CAPABILITIES OF SAMP8 MICE ACCORDING TO THE MWM TEST

Compared with group N, the AD group exhibited reduced learning capability<sup>19</sup>, represented by a

significant prolongation of the escape latency in the PNT from days 1 to 5 ( $P < 0.01$ ) (Fig. 1A, Table 1). After eight acupuncture sessions, group A mice demonstrated a shorter escape latency from days 1 to 3 compared with the AD group, although the difference was not significant ( $P > 0.05$ ). However, the escape latency in group A was significantly shorter on days 4 and 5 ( $P < 0.05$ ) (Fig. 1A, Table 1).

In the SPT, compared with group N, the AD group had a remarkably lower percentage of target quadrant swimming distance and number of effective zone crossings ( $P < 0.01$ ) (Fig. 1B–1C, Table 2), indicating a decrease in memory capacity<sup>19</sup>. However, after acupuncture treatment, both indices were significantly increased compared with those in the AD group ( $P < 0.05$ ) (Fig. 1B–1C, Table 2). In conclusion, the spatial learning and memory capabilities of SAMP8 mice were impaired, which could be improved by acupuncture treatment.

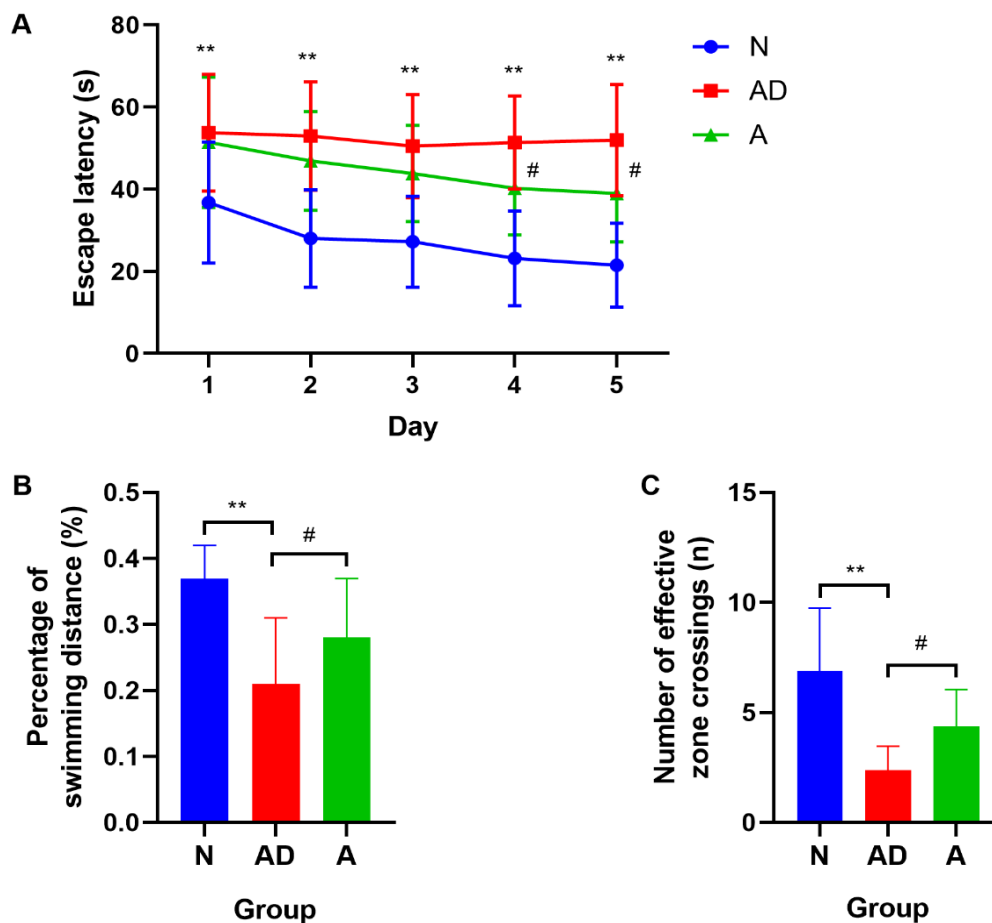


Fig. 1 The learning and memory capabilities of SAMP8 mice. (A) The escape latency. (B, C) The percentage of target quadrant swimming distance and the number of effective zone crossings. (\*\* $P < 0.01$ ; # $P < 0.05$ ). The error bars indicate standard deviation. N, normal group; AD, Alzheimer's disease model group; A, acupuncture treatment group

**Table 1**

The escape latency(s) in PNT from the 1<sup>st</sup> to the 5<sup>th</sup> day among groups.

Group	n	Day1	Day2	Day2	Day4	Day5
N	20	36.79±14.79	28.02±11.85	27.25±11.10	23.14±11.58	21.52±10.25
AD	24	53.74±14.20**	52.97±13.22**	50.49±12.52**	51.39±11.34**	51.97±13.53**
A	19	51.46±15.88	46.88±12.03	43.80±11.80	40.25±11.37#	38.97±11.82#

Note: \*\* $P<0.01$ , group AD vs group N; #  $P<0.05$ , group A vs group AD.

**Table 2**

The percentage of target quadrant swimming distance and the number of crossing effective zone among groups.

Group	n	The percentage of target quadrant swimming distance (%)	The number of crossing effective zone (time)
N	20	0.37±0.05	6.91±2.84
AD	14	0.21±0.10**	2.40±1.07**
A	19	0.28±0.09#	4.38±1.66#

Note: \*\* $P<0.01$ , group AD vs group N; #  $P<0.05$ , group A vs group AD.

#### ACUPUNCTURE HAD A CERTAIN FACILITATIVE EFFECT ON LTP IN SAMP8 MICE

To better understand the effect of acupuncture on synaptic functional plasticity, we evaluated amplitude changes in PS and latency after TS (%), which can reflect changes in synaptic transmission efficacy. The test showed that the PS amplitude in the AD group was slightly higher than that in the N group, but the difference was not significant ( $P>0.05$ ) (Fig. 2A). After acupuncture treatment at GV20 and K11, there was a certain increment in group A compared with that in the AD group, although there was no statistical difference ( $P>0.05$ ) (Fig. 2A–2B). However, there was a significant increase in group A compared with group N (group A vs. group N:  $365.16\pm49.52\%$  vs.  $182.81\pm17.90\%$ ,  $P<0.05$ , Fig. 2A). Additionally, there was a slight increase in the latency amplitude in the AD group compared to that in the N group ( $P>0.05$ ) (Fig. 2C). After acupuncture treatment, it decreased enormously in group A compared with that in groups AD and N (group A vs. group AD:  $85.92\pm2.78\%$  vs.  $105.02\pm2.42\%$ ,  $P<0.05$ ; group A vs. group N:  $85.92\pm2.78\%$  vs.  $93.11\pm1.28\%$ ,  $P<0.05$ , Fig. 2C–2D). This suggests that the synaptic transmission efficacy in the hippocampal DG region

of SAMP8 mice was not altered, but there was a tendency for facilitation. Acupuncture treatment reduced the latency amplitude and increased the PS amplitude, indicating that postsynaptic activity was enhanced during acupuncture treatment, and acupuncture promoted LTP induction.

#### ACUPUNCTURE IMPROVED THE SYNAPTIC ULTRASTRUCTURE OF HIPPOCAMPAL NEURONS OF SAMP8 MICE BASED ON TEM

Compared with group N mice, the PSD thickness (nm) and synaptic interface curvature in group AD mice decreased, and the width of the synaptic cleft (nm) increased significantly ( $P<0.01$ ) (Fig. 3D–3F, Table 3). In group A mice, which received acupuncture treatment, the PSD thickness increased, and the width of the synaptic cleft decreased compared with those in group AD ( $P<0.05$ ) (Fig. 3D–3E, Table 3), although comparison of the synaptic interface curvature showed no significant difference ( $P>0.05$ ) (Fig. 3F). Comparisons of these ultrastructural parameters indicated that there was impairment of synaptic structural plasticity in hippocampal neurons of SAMP8 mice, and this damage could be effectively rectified through acupuncture treatment.

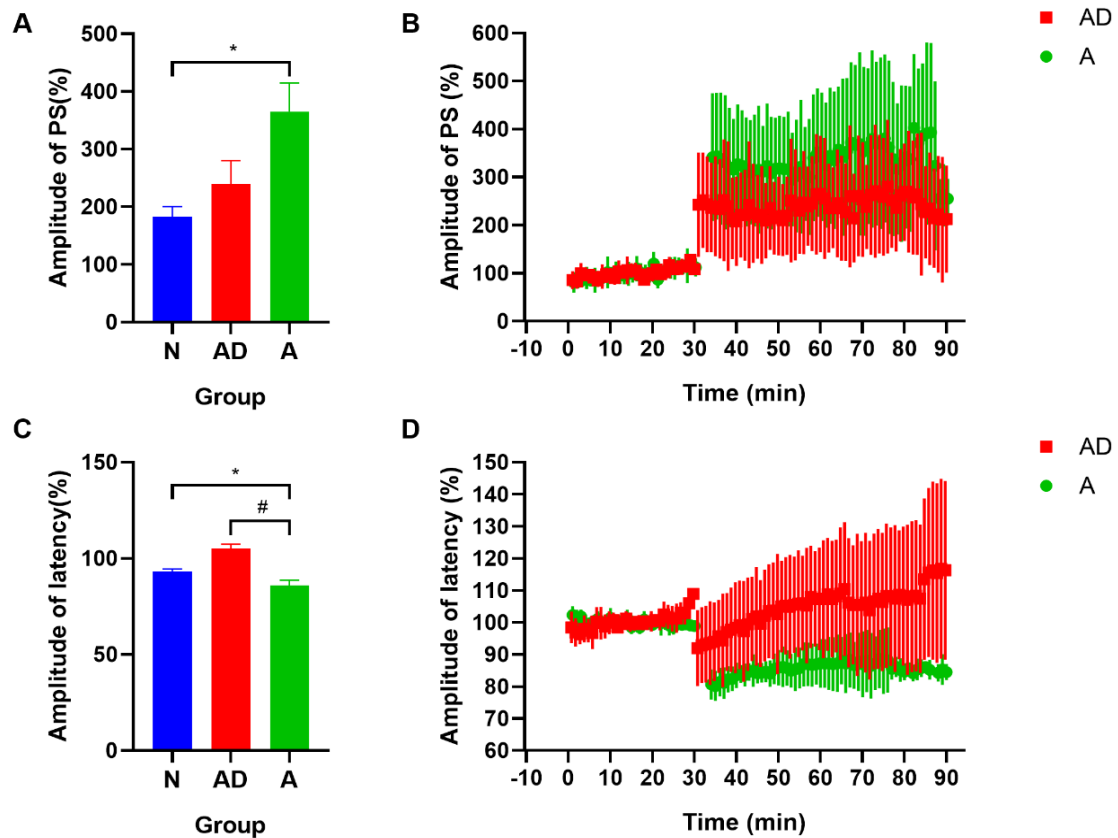


Fig. 2 The hippocampal synaptic functional plasticity of SAMP8 mice. (A, B) The PS amplitude. (C, D) The latency amplitude. (\* $P < 0.05$ ; # $P < 0.05$ ). The error bars indicate standard deviation. PS, population spike; N, normal group; AD, Alzheimer's disease model group; A, acupuncture treatment group

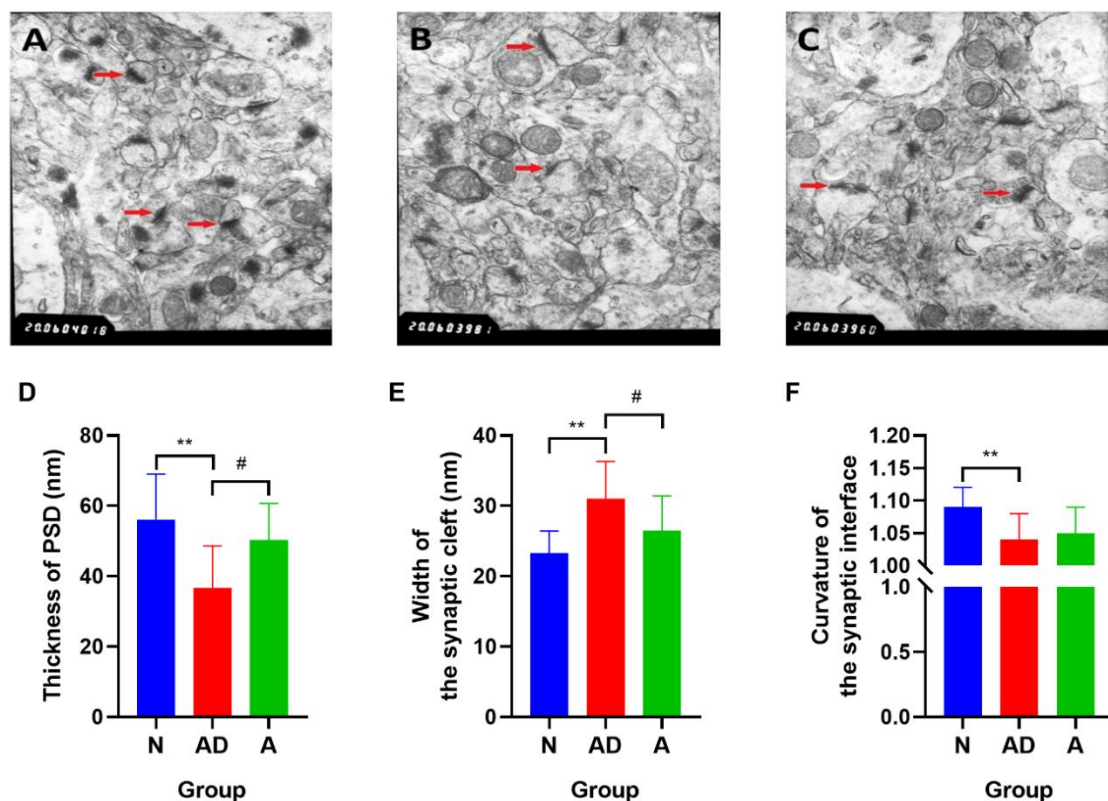


Fig. 3 The synaptic structural plasticity in hippocampal neurons of SAMP8 mice. (A–C) Red arrows represent synapses in the hippocampal CA1 region of mice in groups N, AD, and A, respectively (magnification: 20000). (D–F) The postsynaptic density (PSD) thickness (nm), width of the synaptic cleft, and synaptic interface curvature. (\*\* $P < 0.01$ ; # $P < 0.05$ ). The error bars indicate standard deviation. N, normal group; AD, Alzheimer's disease model group; A, acupuncture treatment group

**Table 3**

The effect of acupuncture treatment on the synaptic ultrastructure of hippocampal neurons in the SAMP8 mice.

Group	n	The PSD thickness (nm)	The width of the synaptic cleft(nm)	The curvature of synaptic interface
N	4	56.18±12.83	23.29±3.16	1.09±0.03
AD	4	36.71±11.94**	31.02±5.29**	1.04±0.04**
A	4	50.29±10.42#	26.53±4.87#	1.05±0.04

Note: \*\* $P < 0.01$ , group AD vs group N; #  $P < 0.05$ , group A vs group AD.

**ACUPUNCTURE REDUCED LACTATE, GLUCOSE, AND PYRUVATE CONTENTS IN THE HIF OF SAMP8 MICE**

To identify metabolism-related factors related to cognitive improvement in SAMP8 mice during acupuncture treatment, glucose, lactate, and pyruvate levels in the HIF were detected using microdialysis. Compared with those in group N, lactate, glucose, and pyruvate levels in the BIF were significantly reduced in the AD group (group AD vs. group N: lactate: 39.84±8.81 μmol/L vs. 72.94±16.35 μmol/L; glucose: 47.69±4.17 μmol/L vs. 63.85±6.67 μmol/L; pyruvate: 4.46±1.16 μmol/L vs 5.53±1.12 μmol/L,

$P < 0.01$ , Fig. 4A–4D). After eight acupuncture treatment sessions, lactate, glucose, and pyruvate concentrations in group A were all prominently decreased compared with those in group AD (group A vs. group AD: lactate: 4.08±1.57 μmol/L vs. 39.84±8.81 μmol/L; glucose: 4.70±0.94 μmol/L vs. 47.69±4.17 μmol/L; pyruvate: 0.84±0.35 μmol/L vs. 4.46±1.16 μmol/L,  $P < 0.01$ , Fig. 4A–4D). This suggests that acupuncture treatment at GV20 and K11 remarkably reduced lactate, glucose, and pyruvate levels in the HIF of SAMP8 mice, and that neuronal uptake of lactate, glucose, and pyruvate in brain intercellular fluid might have been increased.

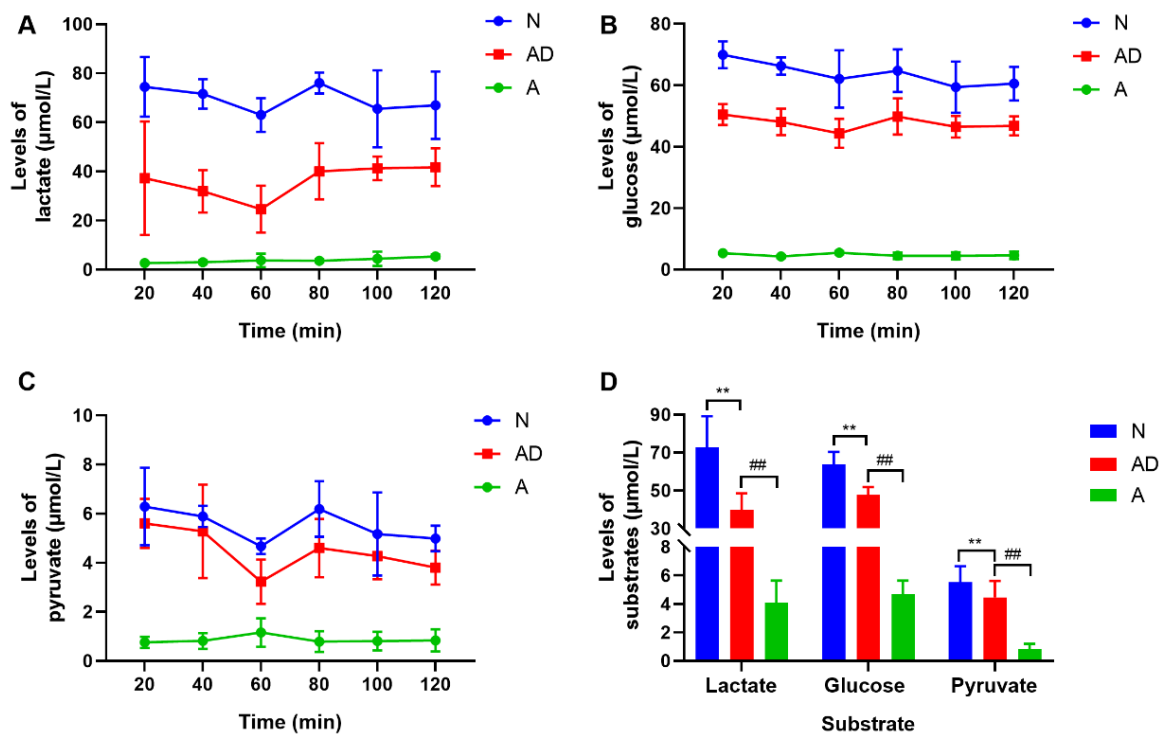


**Fig. 4** The neuronal energy metabolism of SAMP8 mice. (A–C) Changes in lactate, glucose, and pyruvate concentrations in the hippocampal intercellular fluid of each mice group at six different periods during continuous dialysis. (D) The mean levels of substrates. (\*\* $P < 0.01$ , ## $P < 0.01$ ). The error bars indicate standard deviation. N, normal group; AD, Alzheimer’s disease model group; A, acupuncture treatment group



### ACUPUNCTURE ADVANCED GLUT3 AND MCT EXPRESSION IN HIPPOCAMPAL CA1 AND DG REGIONS OF SAMP8 MICE

To further understand the differences in GLUT3, MCT2, and MCT4 expression in various subregions of the hippocampus, the levels of these proteins in the CA1, CA3, and DG regions of the hippocampus were detected using immunohistochemistry. The analysis revealed that the AD group showed reduced GLUT3 levels in the CA1, CA3, and DG regions of the hippocampus in SAMP8 mice compared with those in group N (CA1:  $P<0.01$ ; CA3:  $P<0.05$ ; DG:  $P<0.01$ , Fig. 5A–5B, Table 4). After eight acupuncture treatment courses at GV20 and K11, group A showed increased GLUT3 levels in the CA1 and DG regions compared with those in group AD ( $P<0.01$ ) (Fig. 5A–5B, Table 4), although there was no significant difference in the CA3 region.

Furthermore, the MCT2 level was remarkably reduced in the CA1, CA3, and DG regions of SAMP8 mice compared with that in group N ( $P<0.01$ ) (Fig. 5C–5D, Table 5). After acupuncture treatment at GV20 and K11, group A showed increased MCT2 expression in the CA1 and DG regions compared with that in the AD group (CA1:  $P<0.01$ ; DG:  $P<0.05$ , Fig. 5C–5D, Table 5), although there was no statistical significance in the CA3 region.

Additionally, group AD showed reduced MCT4 levels in the CA1 region of SAMP8 mice, compared with that in group N (group AD vs. group N:  $0.1948\pm 0.0311$  vs.  $0.2608\pm 0.0185$ ,  $P<0.01$ , Fig. 5E–5F), although the changes in the CA3 and DG regions were not statistically significant. After acupuncture treatment, MCT4 expression increased in the CA1 region of SAMP8 mice compared to that in group AD (group A vs. group AD:  $0.2314\pm 0.0364$  vs.  $0.1948\pm 0.0311$ ,  $P<0.05$ , Fig. 5E–5F), although there were no statistical differences in the CA3 and DG regions.

Next, the MOD ratios of MCT4 to MCT2 in the CA1, CA3, and DG regions were compared to understand the outcome of acupuncture treatment on MCT2 and MCT4. The MCT4/MCT2 value in the CA1 region

showed a remarkable difference between groups A and AD (group A vs. group AD:  $0.9792\pm 0.0552$  vs.  $1.1164\pm 0.0931$ ,  $P<0.05$ , Fig. 5G). However, the discrepancies in the other groups and regions were not statistically significant.

In summary, acupuncture facilitated GLUT3 and MCT2 expression in the CA1 and DG subregions of SAMP8 mice, and the regulatory effect on MCT4 was mainly in the CA1 region. A comparison of the MCT4/MCT2 values in the CA1 region suggested that acupuncture treatment elevated MCT2 more significantly than MCT4, indicating that the effect of acupuncture on neurons was more remarkable.

### ACUPUNCTURE ENHANCED GLUT3 AND MCT2 EXPRESSION IN THE HIPPOCAMPUS OF SAMP8 MICE

Since the level of energy substrate transport proteins directly affects the energy substrate contents in HIF, the total expression of GLUT3, MCT2, and MCT4 in the hippocampus of each mice group was evaluated using western blotting. The expression of GLUT3, MCT2, and MCT4 in the hippocampus of SAMP8 mice was lower than those in group N (group AD vs. group N; GLUT3:  $0.26\pm 0.07$  vs.  $0.52\pm 0.09$ ,  $P<0.01$ ; MCT2:  $0.57\pm 0.13$  vs.  $0.89\pm 0.09$ ,  $P<0.01$ ; MCT4:  $0.45\pm 0.12$  vs.  $0.53\pm 0.13$ ,  $P<0.05$ , Fig. 6A–6B). Additionally, the levels of GLUT3 and MCT2 proteins increased noticeably after eight acupuncture treatment courses (group A vs. group AD; GLUT3:  $0.41\pm 0.11$  vs.  $0.26\pm 0.07$ ,  $P<0.01$ ; MCT2:  $0.76\pm 0.11$  vs.  $0.57\pm 0.13$ ,  $P<0.01$ , Fig. 6A–6B), whereas there was no change in MCT4 ( $P>0.05$ ). These findings confirmed that acupuncture treatment was effective in boosting GLUT3 and MCT2 expression in the hippocampus of SAMP8 mice.

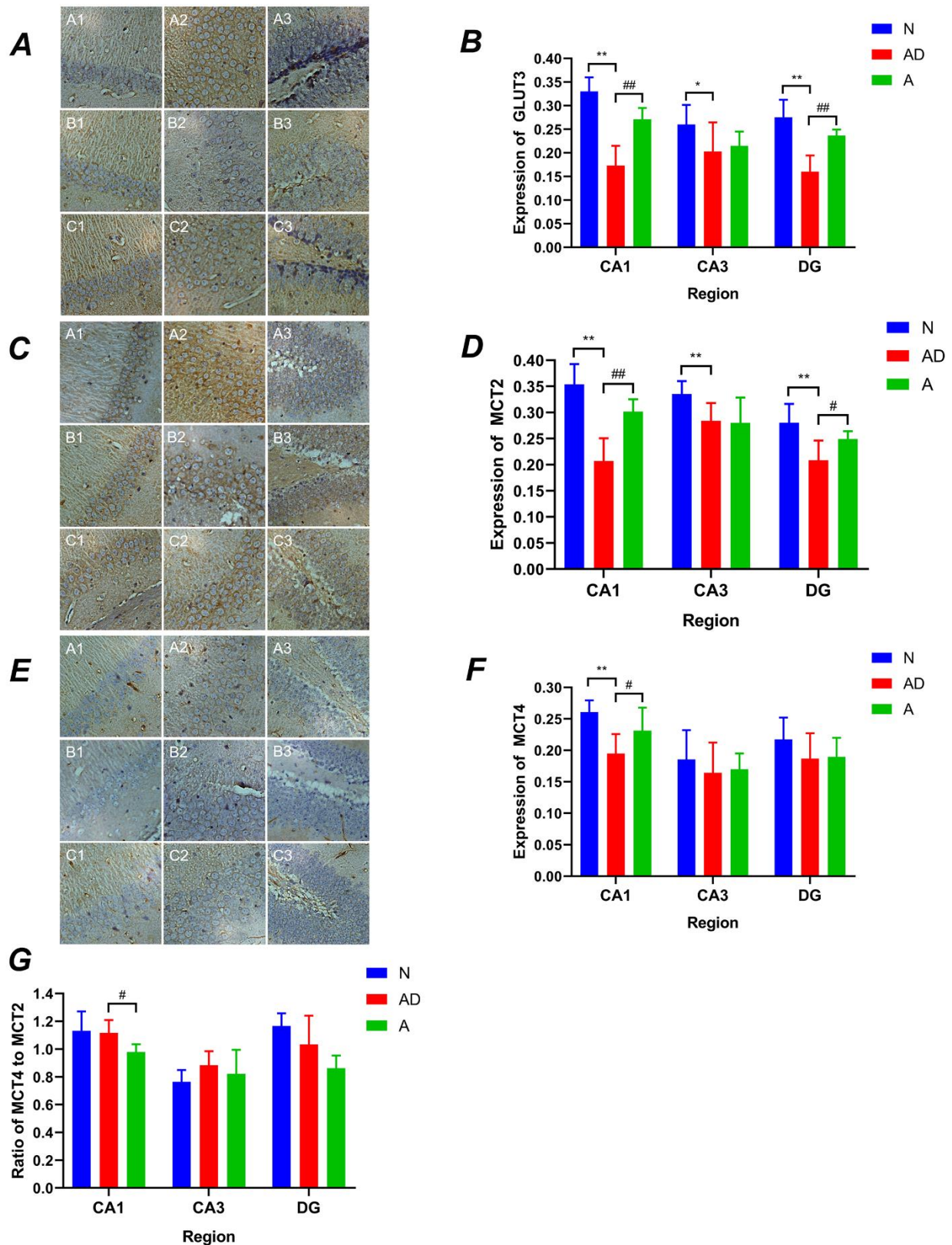


Fig. 5 The GLUT3 and monocarboxylate transporter (MCT) expression in the hippocampal regions of SAMP8 mice. (A, B) A1–A3 present GLUT3 expression in the hippocampal CA1, CA3, and DG regions of group N mice (400X microscope), B1–B3 present GLUT3 expression in the hippocampal CA1, CA3, and DG regions for group AD, C1–C3 present GLUT3 expression in the hippocampal CA1, CA3, and DG regions of group A mice. (C, D) and (E, F) represent MCT2 and MCT4, respectively. (G) The MCT4/MCT2 value in the hippocampal regions for groups N, AD and A. (\*\* $P < 0.01$ , \* $P < 0.05$ , ## $P < 0.01$ , # $P < 0.05$ ). The error bars indicate standard deviation. N, normal group; AD, Alzheimer’s disease model group; A, acupuncture treatment group

**Table 4**

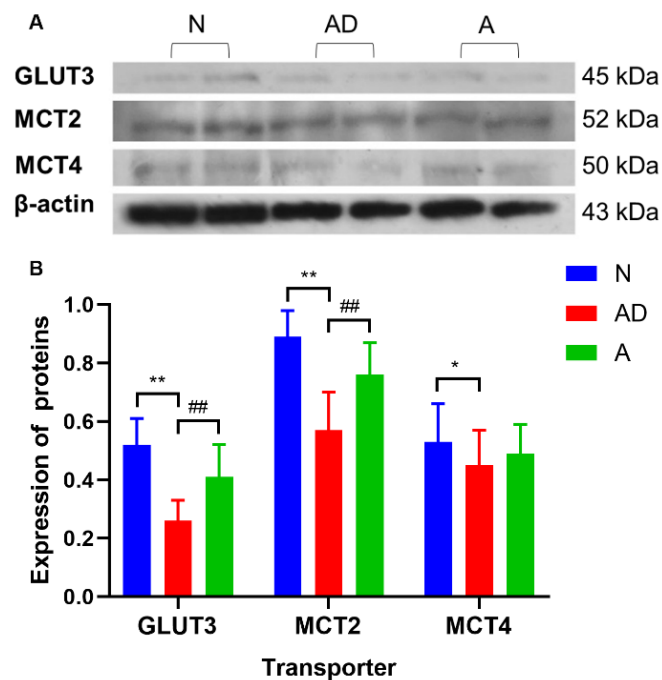
The level of GLUT3 in the hippocampal CA1, CA3 and DG regions of each group of the mice.

Group	n	CA1	CA3	DG
N	7	0.3303±0.0296	0.2602±0.0412	0.275±0.0374
AD	6	0.1728±0.0424**	0.2029±0.0615*	0.1603±0.0342**
A	7	0.2713±0.0239##	0.2148±0.0303	0.2367±0.0128##

Note: \*\* $P<0.01$ , \* $P<0.05$ , group AD vs group N; ##  $P<0.01$ , group A vs group AD.**Table 5**

The level of MCT2 in the hippocampal CA1, CA3 and DG regions of each group of the mice.

Group	n	CA1	CA3	DG
N	7	0.3538±0.0389	0.3354±0.0249	0.2805±0.0359
AD	6	0.2073±0.0436**	0.2841±0.0341**	0.2086±0.0376**
A	7	0.3019±0.0237##	0.2803±0.0482	0.2492±0.0151#

Note: \*\* $P<0.01$ , group AD vs group N; ##  $P<0.01$ , #  $P<0.05$ , group A vs group AD.

**Fig. 6** The GLUT3 and monocarboxylate transporter (MCT) expression in the hippocampus of SAMP8 mice. (A) The clear protein bands of hippocampal GLUT3, MCT2, and MCT4 in different groups and their comparisons with the internal reference of  $\beta$ -actin can be seen. (B) GLUT3, MCT2, and MCT4 expression in the hippocampus. (\*\* $P<0.01$ , \* $P<0.05$ , ## $P<0.01$ ). The error bars indicate standard deviation. N, normal group; AD, Alzheimer's disease model group; A, acupuncture treatment group

## Discussion

### SYNAPTIC PLASTICITY OF HIPPOCAMPAL NEURONS AND LEARNING AND MEMORY CAPACITIES

In this study, the SAMP8 mouse was selected as an AD model because it shows the rapid aging characteristics

of AD and typical pathological changes in the CNS<sup>24</sup>. As an important brain region responsible for learning and memory, the hippocampus is involved in the acquisition and maintenance of declarative memory<sup>25</sup>, which we examined using the MWM test in this study. Therefore, the decline in MWM performance in SAMP8 mice was consistent with impairment of

learning and memory competence in AD. The hippocampus is the first brain region to be damaged in AD, including the hippocampal CA1, CA3, and DG subregions, but the CA1 region is most seriously impaired<sup>2,26,27</sup>. The synaptic plasticity of hippocampal neurons is crucial for the formation of learning and memory, especially LTP, which is the physiological basis for learning and memory<sup>28</sup>. Damage to the synaptic structure and functional plasticity caused by reduced numbers, altered morphological structure, and dysfunctional transmission of synapses is an important manifestation of hippocampal neuron injury and a crucial pathological mechanism of AD<sup>3,4</sup>. Thus, TEM observation showed that the PSD thickness and synaptic interface curvature decreased, and the width of the synaptic cleft increased in the hippocampal CA1 region of SAMP8 mice, indicating that synaptic structural plasticity was indeed damaged in AD.

Synaptic functional plasticity is reflected in the enhancement and weakening of synaptic transmission efficiency, including LTP and long-term depression<sup>28</sup>. LTP is a major electrophysiological indicator of synaptic plasticity<sup>29</sup>. Synaptic structural and functional plasticity are based on and influence each other. Impairment of synaptic structural plasticity triggers a reduction in synaptic transmission efficiency. However, the LTP experiment results in this study showed that the amplitude changes of PS and the latency after TS in SAMP8 mice were not significantly different from those in SAMR1 mice, indicating that the synaptic transmission efficacy of the PP-DG pathway was not significantly changed. Several factors contributed to this inconsistency. The first is the differences in the hippocampal subregions. Each subregion has different physicochemical properties and is involved in learning memory function to different degrees<sup>30</sup>; thus, there are differences in AD susceptibility among the subregions. The dorsal hippocampus mainly occupies the CA1 area, and is closely associated with learning and memory<sup>31</sup>, while the ventral hippocampus mainly covers the DG area, is more relevant to emotional stress, and is one of the key areas of emotional memory<sup>32,33</sup>.

Although AD may involve the entire hippocampus, the CA1 region is the earliest and most seriously damaged<sup>2</sup>. Therefore, atrophy of the CA1 region is suggested to be an important biomarker for the preclinical stages of AD<sup>27</sup>. In contrast, the postsynaptic responses recorded in vivo in this study were from the DG area, which may be an important reason for the discrepancy between the LTP results and those of the MWM and TEM experiments. Additionally, this may be related to the age of mice. An LTP study showed that the PS amplitude of SAMR1 mice increased and then decreased with age, while the PS amplitude of SAMP8 mice continued to decrease<sup>34</sup>; thus, we could conclude that there was no significant difference in the PS amplitude between 8-month-old SAMR1 and SAMP8 mice. Additionally, the stronger immune function in SAMR1 mice led to an enhanced acute inflammatory response in the brain tissue during LTP measurement, while excessive inflammatory factors inhibited LTP<sup>34</sup>. Meanwhile, SAMR1 mice, which are normal mice, may be more responsive to the condition of fester, and this stress had an impact on the LTP results. Furthermore, the relationship between hippocampal tertiary synapses and primary and secondary synapses is not a simple linear one<sup>30</sup>; thus, the electrophysiological record of the primary synaptic pathway PP-DG may not reflect the synaptic transmission efficiency of the downstream CA1 region. Nevertheless, the LTP test in this study revealed a tendency of LTP facilitation evoked by the PP-DG pathway in SAMP8 mice, but the difference was not statistically significant, which may be due to the small sample size in this study. Thus, there is no evidence that SAMP8 mice do not experience impairments in synaptic functional plasticity.

After acupuncture treatment at acupoints GV20 and K11, mice showed enhanced learning and memory capabilities, increased PSD thickness, reduced synaptic cleft width in hippocampal neurons, increased PS amplitude, and shortened latency amplitude. These results confirmed that postsynaptic activity and synaptic transmission efficacy were promoted by acupuncture treatment.

Although the change in the PS amplitude was not significant, it confirmed that acupuncture facilitates TS-induced hippocampal synaptic LTP. These results were also confirmed by previous studies<sup>14,15,20,35,36</sup>. Consequently, we can conclude that acupuncture promotes spatial learning and memory capabilities of SAMP8 mice by improving synaptic structural plasticity of hippocampal neurons.

#### ENERGY METABOLISM OF HIPPOCAMPAL NEURONS AND SYNAPTIC PLASTICITY

In the CNS, energy substrates such as glucose, lactate, and pyruvate cannot pass freely through the cell membrane, and must rely on GLUTs and MCTs to enter the BIF from the blood and eventually be taken up by neurons<sup>7,11</sup>. GLUT3 is a neuron-specific glucose transporter with a high affinity for glucose, and is crucial for glucose uptake by neurons<sup>12</sup>. MCTs are responsible for the transportation of monocarboxylic acids, such as lactate and pyruvate, of which MCT4 is mainly expressed in astrocytes, whereas MCT2 is primarily expressed in neurons<sup>11</sup>. Additionally, MCT2 is also expressed on the postsynaptic membrane and postsynaptic densities of hippocampal and cerebellar glutamatergic synapses, suggesting a close relationship between MCT2 and synaptic plasticity<sup>37</sup>. Therefore, the concentration of energy substrates in HIF is closely related to these transporters. When glucose and lactate are present together, neurons preferentially oxidize lactate<sup>38</sup>. Since lactate does not readily cross the blood-brain barrier, lactate in the blood is not the primary source of lactate in the CNS, but rather in the astrocytes<sup>39</sup>. Astrocytes are the main site for glycogen storage and lactate production, but uptake and utilization of lactate occur in neurons; thus, a lactate transport system must exist between astrocytes and neurons. Astrocytes take up 80% of the glucose in the blood and convert it into lactate, which is transported extracellularly via MCT4 and then intracellularly via MCT2 to the neuron for neuronal energy consumption<sup>39,40,41</sup>. Lactate transportation between astrocytes and neurons is essential for maintaining LTP and forming long-term memory<sup>9</sup>, and is critical for energy metabolism in

the pathophysiological states of the nervous system<sup>10</sup>.

In this study, we found that the levels of lactate, glucose, and pyruvate in the BIF of SAMP8 mice decreased remarkably, indicating that the source of these substances in the BIF is insufficient and that impaired neuronal energy metabolism is a fundamental pathological feature of AD, which is consistent with other reports<sup>7,11,42</sup>. Moreover, GLUT3 and MCT2 expression in the hippocampal CA1, CA3, and DG subregions and MCT4 expression in the CA1 region was significantly reduced in SAMP8 mice, indicating a general impairment in the uptake of energy substrates by hippocampal neurons. This served as another piece of evidence regarding the decrease in lactate, glucose, and pyruvate contents in the BIF of SAMP8 mice. We also found that the transmembrane transportation of lactate between astrocytes and neurons was reduced, which led to the impairment of energy supply to neurons, synaptic plasticity function, and learning and memory capabilities. Therefore, impairment of synaptic structural plasticity in the hippocampal CA1 region and deterioration of MWM performance in SAMP8 mice were observed in the TEM and MWM experiments. However, after eight sessions of effective acupuncture treatment at GV20 and K11, lactate, glucose, and pyruvate levels in the BIF were significantly reduced from previous levels, which seemed to be contradictory to the improvement of learning and memory capabilities as well as the synaptic structural plasticity in the mice after acupuncture treatment. In this study, there were several reasons for this finding. First, the substrate source in the BIF itself was reduced due to the rapid aging process of SAMP8 mice, and 8 weeks of acupuncture treatment could improve, but not reverse, the aging process and increase the substrate source in the BIF. Second, GLUT3 and MCT2 expression in the hippocampal CA1 and DG regions increased remarkably after acupuncture treatment, suggesting an increased uptake of lactate, glucose, and pyruvate in the BIF by neurons. Finally, the immunohistochemistry experiment showed a

modulatory effect of acupuncture on MCT4; therefore, we could conclude that MCT4 enhanced lactate transportation between astrocytes and neurons, and promoted the ability to store and match substrates. MCT2 had the highest affinity for lactate, whereas MCT4 had the lowest. MCT2 is saturated at low concentrations, whereas MCT4 is less susceptible to saturation and has a higher transporter space and efficiency<sup>43,44</sup>. Consequently, a slight modulation of MCT4 by acupuncture will significantly impact lactate supply to neurons. Additionally, microdialysis was performed during the day when mice were in the glycogen reserve stage in the brain, which also provided a basis for lactate reduction in the HIF<sup>45</sup>.

In summary, the hippocampal CA1 and DG subregions are the main regions regulated by acupuncture treatment, whereas neurons are the main targets of action. By producing optimal effects on multiple links of energy substrate transportation in the brain of SAMP8 mice, acupuncture treatment provides energy for synaptic plasticity and functional neuronal activity, and ultimately has positive effects on learning and memory capabilities. Nevertheless, this study had some limitations. First, our study only investigated GLUT3, MCT2, and MCT4 expression, and did not address other substances related to energy metabolism. Second, whether the substrate transportation of energy metabolism and the role of astrocytes in neuronal energy metabolism is crucial in promoting synaptic plasticity of hippocampal neurons by acupuncture was not examined. Third, this study did not explore how acupuncture treatment regulates GLUT3, MCT2, and MCT4; this will be investigated in the next stage of this research.

## Conclusion

Acupuncture can improve spatial learning and memory capabilities, as well as hippocampal synaptic plasticity in SAMP8 mice. Possible mechanisms for this are remodeling of neuronal energy metabolism disorders, which increase the energy substrate reserve of neurons and improve the substrate-matching ability of cellular response by regulating the expression of neuron-specific GLUT3 and MCT2

and astrocyte-specific MCT4 in the hippocampal CA1 and DG regions. We hope that our study will provide new ideas and experimental evidence for the study of mechanisms of acupuncture-promoted nerve rehabilitation, and serve as the groundwork for further studies of acupuncture-induced synaptic plasticity.

## Conflicts of Interest Statement:

The authors have no competing conflicts of interest to declare.

## Acknowledgements:

The authors thank Prof. Yubing Shi and Haifa Qiao for their critical reading of the manuscript.

## Funding Statement:

This work was financially supported by the National Natural Science Foundation of China (grant numbers 82074567, 81904311, and 81873386) and the Natural Science Foundation of Shaanxi (grant number 2017JQ8020).

## Author contributions:

Min Feng, Shuguang Yu, and Qi Liu conceived and designed the experiments. Qi Liu, Ping Du, Min Feng, Xiaoshu Zhang, Changle Wu, Li Zhang, and Yiyun Yuan performed the experiments. Changle Wu, Mengjing Wang, and Xiaoshu Zhang analyzed the images and data. Changle Wu and Mengjing Wang drafted the manuscript. All the authors approved the final version of the manuscript.

## Ethical approval of studies:

The animal study was reviewed and approved by the Ethics Committee of Shaanxi University of Chinese Medicine, China.

## Data sharing statement:

The data in this study is available from the corresponding author upon reasonable request.

## References:

1. Long JM, Holtzman DM. Alzheimer Disease: An Update on Pathobiology and Treatment Strategies. *Cell*. 2019;179(2):312-339. Doi: 10.1016/j.cell.2019.09.001
2. Counts SE, Alldred MJ, Che S, Ginsberg SD, Mufson EJ. Synaptic gene dysregulation within hippocampal CA1 pyramidal neurons in mild cognitive impairment. *Neuropharmacology*. 2014; 79:172-179. Doi: 10.1016/j.neuropharm.2013.10.018
3. Selkoe DJ. Alzheimer's disease is a synaptic failure. *Science*. 2002;298(5594):789-791. Doi: 10.1126/science.1074069
4. Puzzo D, Piacentini R, Fá M, Gulisano W, Li PD, Staniszewski A, et al. LTP and memory impairment caused by extracellular A $\beta$  and Tau oligomers is APP-dependent. *Elife*. 2017;6: e26991. Doi: 10.7554/eLife.26991
5. Blandini F, Braunevel KH, Manahan-Vaughan D, Orzi F, Sarti P. Neurodegeneration and energy metabolism: from chemistry to clinics. *Cell Death Differ*. 2004;11(4):479-484. Doi: 10.1038/sj.cdd.4401323
6. Caspersen C, Wang N, Yao J, Sosunov A, Chen X, Lustbader JW, et al. Mitochondrial A $\beta$ : a potential focal point for neuronal metabolic dysfunction in Alzheimer's disease. *FASEB J*. 2005; 19(14):2040-2041. Doi: 10.1096/fj.05-3735fje
7. An Y, Varma VR, Varma S, Casanova R, Dammer E, Pletnikova O, et al. Evidence for brain glucose dysregulation in Alzheimer's disease. *Alzheimers Dement*. 2018;14(3):318-329. Doi: 10.1016/j.jalz.2017.09.011
8. Magistretti PJ, Pellerin L, Rothman DL, Shulman RG. Energy on demand. *Science*. 1999;283 (5401):496-497. Doi: 10.1126/science.283.5401.496
9. Suzuki A, Stern SA, Bozdagi O, Huntley GW, Walker RH, Magistretti PJ, et al. Astrocyte-neuron lactate transport is required for long-term memory formation. *Cell*. 2011;144(5):810-823. Doi: 10.1016/j.cell.2011.02.018
10. Mason S. Lactate Shuttles in Neuroenergetics-Homeostasis, Allostasis and Beyond. *Front Neurosci*. 2017; 11(43):1-15. Doi: 10.3389/fnins.2017.00043
11. Netzahualcoyotzi C, Pellerin L. Neuronal and astroglial monocarboxylate transporters play key but distinct roles in hippocampus-dependent learning and memory formation. *Prog Neurobiol*. 2020; 194:101888. Doi: 10.1016/j.pneurobio.2020.101888
12. Szablewski L. Brain Glucose Transporters: Role in Pathogenesis and Potential Targets for the Treatment of Alzheimer's Disease. *Int J Mol Sci*. 2021;22(15):8142. Doi: 10.3390/ijms22158142
13. Contreras-Baeza Y, Sandoval PY, Alarcón R, Galaz A, Cortes-Molina F, Alegria K, et al. Monocarboxylate transporter 4 (MCT4) is a high affinity transporter capable of exporting lactate in high-lactate microenvironments. *J Biol Chem*. 2019;294(52):20135-20147. Doi: 10.1074/jbc.RA119.009093
14. Peng J, Zeng F, He YH, Tang Y, Yin HY, Yu SG. Study on the effect of electroacupuncture on mitochondria in the hippocampus of SAMP8 mice, *Acupuncture Research (Chin)*. 2007;32 (6) 364-367. Doi: CNKI: SUN: XCYJ.0.2007-06-004.
15. Wu QF, Guo LL, Yu SG, Zhang Q, Lu SF, Zeng F, et al. A (1)H NMR-based metabolomic study on the SAMP8 and SAMR1 mice and the effect of electro-acupuncture. *Exp Gerontol*. 2011;46(10): 787-793. Doi: 10.1016/j.exger.2011.06.002
16. Wang YY, Yu SF, Xue HY, Li Y, Zhao C, Jin YH, et al. Effectiveness and Safety of Acupuncture for the Treatment of Alzheimer's Disease: A Systematic Review and Meta-Analysis. *Front Aging Neurosci*. 2020;12(98):1-21. Doi: 10.3389/fnagi.2020.00098
17. Yu CC, Du YJ, Wang SQ, Liu LB, Shen F, Wang L, et al. Experimental Evidence of the Benefits of Acupuncture for Alzheimer's Disease: An Updated Review. *Front Neurosci*. 2020; 14:549772. Doi: 10.3389/fnins.2020.549772
18. Xie LS, Liu Y, Zhang N, Li CY, Aaron FS, George W, et al. Electroacupuncture Improves M2

- Microglia Polarization and Glia Anti-inflammation of Hippocampus in Alzheimer's Disease. *Front Neurosci.* 2021; 15:689629. Doi: 10.3389/fnins.2021.689629
19. Vorhees CV, Williams MT. Morris water maze: procedures for assessing spatial and related forms of learning and memory. *Nat Protoc.* 2006;1(2):848-858. Doi: 10.1038/nprot.2006.116
20. Shen MH, Tang QQ, Li ZR, Ma P. Effects of electroacupuncture on long-term potentiation of hippocampus in a rat model of Alzheimer's disease induced by A $\beta$  (25-35). *Acupuncture Research (Chin).* 2010;35(01):3-7. Doi:10.13702/j.1000-0607.2010.01.011.
21. Paxinos G, Franklin KBJ. The mouse brain in stereotaxic coordinates. *Academic Press.* San Diego. 1997: 186.
22. Jones DG, Calverley RK. Frequency of occurrence of perforated synapses in developing rat neocortex. *Neurosci Lett.* 1991;129(2):189-192. Doi: 10.1016/0304-3940(91)90458-6
23. Jones DG, Devon RM. An ultrastructural study into the effects of pentobarbitone on synaptic organization. *Brain Res.* 1978;147(1):47-63. Doi : 10.1016/0006-8993 (78) 90771-0
24. Liu B, Liu J, Shi JS. SAMP8 Mice as a Model of Age-Related Cognition Decline with Underlying Mechanisms in Alzheimer's Disease. *J Alzheimers Dis.* 2020;75(2):385-395. Doi: 10.3233/JAD-200063
25. Jahn H. Memory loss in Alzheimer's disease. *Dialogues Clin Neurosci.* 2013;15(4):445-454. Doi : 10.31887/DCNS.2013.15.4/hjahn
26. Kelleher-Andersson J. Discovery of neurogenic, Alzheimer's disease therapeutics. *Curr Alzheimer Res.* 2006;3(1):55-62. Doi: 10.2174/156720506775697179
27. Apostolova LG, Mosconi L, Thompson PM, Green AE, Hwang KS, Ramirez A, et al. Subregional hippocampal atrophy predicts Alzheimer's dementia in the cognitively normal. *Neurobiol Aging.* 2010; 31(7):1077-1088. Doi: 10.1016/j.neurobiolaging.2008.08.008
28. Nabavi S, Fox R, Proulx CD, Lin JY, Tsien RY, Malinow R. Engineering a memory with LTD and LTP. *Nature.* 2014;511(7509):348-352. Doi: 10.1038/nature13294
29. Bliss TV, Collingridge GL. A synaptic model of memory: long-term potentiation in the hippocampus. *Nature.* 1993;361(6407):31-39. Doi: 10.1038/361031a0
30. Scullin CS, Partridge LD. Modulation by pregnenolone sulfate of filtering properties in the hippocampal trisynaptic circuit. *Hippocampus.* 2012;22(11):2184-2198. Doi: 10.1002/hipo.22038
31. Yiu AP, Rashid AJ, Josselyn SA. Increasing CREB function in the CA1 region of dorsal hippocampus rescues the spatial memory deficits in a mouse model of Alzheimer's disease. *Neuropsychopharmacology.* 2011;36(11):2169-2186. Doi: 10.1038/npp.2011.107
32. Tanti A, Belzung C. Neurogenesis along the septo-temporal axis of the hippocampus: are depression and the action of antidepressants region-specific. *Neuroscience.* 2013; 252:234-252. Doi: 10.1016/j.neuroscience.2013.08.017
33. Redondo RL, Kim J, Arons AL, Ramirez S, Liu X, Tonegawa S. Bidirectional switch of the valence associated with a hippocampal contextual memory engram. *Nature.* 2014;513(7518):426-430. Doi: 10.1038/nature13725
34. Huang Y. Preliminary study on the relationship between immune function status and LTP and the mechanism of puzzling effect of Liu Wei Di Huang Tang and its active ingredient CA4-3. *Chinese People's Liberation Army Academy of Military Medical Sciences.* 2009:127.
35. Lu SF, Shao X, Tang Y, Yin HY, Chen J, Yu SG. Mechanism of neural cell adhesion in hippocampal neuronal synaptic plasticity in mice with Alzheimer's disease model (SAMP8) promoted by electroacupuncture. *Chinese Journal of Rehabilitation Medicine (Chin).*2008;23(12):1057-1060. Doi: CNKI: SUN: ZGKF.0.2008-12-003.
36. Yang G, Pei YN, Shao SJ, Gao YS, Zhang SJ, Hu C. Effects of electroacupuncture at "Baihui" and



- “Yongquan” points on the expression of synaptic plasticity-related proteins in the hippocampus of app/ps1 double transgenic mice. *Acupuncture Research (Chin)*.2020;45(04):310-314. Doi:10.13702/j.1000-0607.190012.
37. Bergersen LH, Magistretti PJ, Pellerin L. Selective postsynaptic co-localization of MCT2 with AMPA receptor GluR2/3 subunits at excitatory synapses exhibiting AMPA receptor trafficking. *Cereb Cortex*. 2005;15(4):361-370. Doi: 10.1093/cercor/bhh138
38. Bouzier-Sore AK, Voisin P, Canioni P, Magistretti PJ, Pellerin L. Lactate is a preferential oxidative energy substrate over glucose for neurons in culture. *J Cereb Blood Flow Metab*. 2003;23(11):1298-1306. Doi: 10.1097/01.WCB.0000091761.61714.25
39. Pellerin L, Magistretti PJ. How to balance the brain energy budget while spending glucose differently. *J Physiol*. 2003;546(Pt 2):325. Doi: 10.1113/jphysiol.2002.035105
40. Zwingmann C, Leibfritz D. Regulation of glial metabolism studied by <sup>13</sup>C-NMR. *NMR Biomed*. 2003;16(6-7):370-399. Doi: 10.1002/nbm.850
41. Mächler P, Wyss MT, Elsayed M, Stobart J, Gutierrez R, von Faber-Castell A, et al. In Vivo Evidence for a Lactate Gradient from Astrocytes to Neurons. *Cell Metab*. 2016;23(1):94-102. Doi: 10.1016/j.cmet.2015.10.010
42. Lu W, Huang J, Sun S, Huang S, Gan S, Xu J, et al. Changes in lactate content and monocarboxylate transporter 2 expression in A $\beta$ <sub>25-35</sub>-treated rat model of Alzheimer’s disease. *Neurol Sci*. 2015; 36(6):871-876. Doi: 10.1007/s10072-015-2087-3
43. Manning Fox JE, Meredith D, Halestrap AP. Characterisation of human monocarboxylate transporter 4 substantiates its role in lactic acid efflux from skeletal muscle. *J Physiol*. 2000;529(Pt 2):285-293. Doi: 10.1111/j.1469-7793.2000.00285.x
44. Hertz L, Dienel GA. Lactate transport and transporters: general principles and functional roles in brain cells. *J Neurosci Res*. 2005;79(1-2):11-18. Doi: 10.1002/jnr.20294
45. Petit JM, Tobler I, Kopp C, Morgenthaler F, Borbély AA, Magistretti PJ. Metabolic response of the cerebral cortex following gentle sleep deprivation and modafinil administration. *Sleep*. 2010;33(7):901-908. Doi: 10.1093/sleep/33.7.901